Published in final edited form as:
Cancer Genet. 2013 ; 206(0): 1–11. doi:10.1016/j.cancergen.2012.12.004.

A Novel 4-color Fluorescence in Situ Hybridization Assay for Detection of *TMPRSS2* and *ERG* Rearrangements in Prostate Cancer

Xiaoyu Qu[a], **Grace Randhawa**[b], **Cynthia Friedman**[b], **Siobhan O'Hara-Larrivee**[b], **Kathleen Kroeger**[b], **Ruth Dumpit**[a], **Larry True**[c], **Funda Vakar-Lopez**[c], **Christopher Porter**[d], **Robert Vessella**[c,e], **Peter Nelson**[a,c], and **Min Fang**[a,b,c]

[a]Fred Hutchinson Cancer Research Center, Seattle, WA

[b]Seattle Cancer Care Alliance, Seattle, WA

[c]University of Washington, Seattle, WA

[d]Virginia Mason Medical Center, Seattle, WA

[e]Puget Sound VA Health Care System

Abstract

Purpose—Since the identification of *TMPRSS2/ERG* rearrangement as the most common fusion event in prostate cancer, various methods have been developed to detect this rearrangement and to study its prognostic significance. We hereby report a novel 4-color fluorescence in situ hybridization (FISH) assay that not only detects the typical *TMPRSS2:ERG* fusion but also alternative rearrangements of either the *TMPRSS2* or *ERG* gene.

Experimental design—We validated this assay on fresh, frozen, or formalin-fixed paraffin-embedded prostate cancer specimens including cell lines, primary prostate cancer, xenograft tissues derived from metastatic prostate cancer, and metastatic tissues from castration-resistant prostate cancer (CRPC) patients.

Results—When compared with RT-PCR or Gen-Probe method as the technical reference, the 4-color FISH assay demonstrated an analytical sensitivity of 94.5% (95% Confidence Interval [CI] 0.80-0.99) and specificity of 100% (95% CI 0.89-1.00) for detecting *TMPRSS2:ERG* fusion. *TMPRSS2:ERG* fusion was detected at 41% and 43% in primary prostate cancer (n = 59) and CRPC tumors (n = 82), respectively. Alternative rearrangements other than the typical *TMPRSS2:ERG* fusion were confirmed by karyotype analysis and shown present in 7% primary cancer and 13% CRPC tumors. Successful karyotype analysis is reported for the first time on four of the xenograft samples, complementing the FISH results.

Conclusions—This 4-color FISH assay provides sensitive detection of *TMPRSS2* and *ERG* gene rearrangements in prostate cancer.

Corresponding author: Min Fang, M.D., Ph.D., FACMG Fred Hutchinson Cancer Research Center 825 Eastlake Ave. E., G7-500 Seattle, WA 98109-1023 phone: (206) 288-1385 Fax: (206)288-7567 mfang@fhcrc.org.

There is no conflict of interest to disclose.

Keywords

Prostate cancer; TMPRSS2; ERG; FISH

Introduction

The chromosomal rearrangements involving androgen-regulated *TMPRSS2* and ETS transcription factors present great potential as prognostic markers for human prostate cancer due to their biological relevance, prevalence among prostate cancer patients, specificity to the disease, and underlying molecular mechanisms influencing cellular phenotypes (1). Identification of these rearrangements may allow for stratification of prostate cancers into subtypes that respond to specific therapeutics (2). The most common type of rearrangement involves the fusion of *TMPRSS2* to oncogene *ERG* due to the deletion of intervening genomic sequences on chromosome 21 or insertion of this sequence to separate location(s) of the genome (3, 4), which leads to high levels of *ERG* expression. *TMPRSS2:ERG* fusion demonstrates high prevalence and specificity in prostate cancer, such that it has been detected in nearly half of the prostate cancer patients but none of the benign prostate tissues (5-9).

Despite the great interest in clinical significance of the *TMPRSS2:ERG* fusion, studies on its relevance to disease outcome have yielded discordant conclusions. The inconsistency can be attributed to multiple factors such as the different patient cohort, the determination of study end point, and the technique used to detect *TMPRSS2/ERG* rearrangement (7). Among the technologies for the detection of gene rearrangements, fluorescence in situ hybridization (FISH) remains the most robust method to date in the analysis of archived clinical samples that are formalin-fixed and paraffin-embedded (FFPE). Of note, the recent development of anti-ERG monoclonal antibodies has further enhanced the detection of ERG overexpression in *ERG*-rearranged tissues, particularly in FFPE samples (10, 11). In FISH characterized cohorts, these antibodies have shown remarkable correlation between ERG rearrangement and protein expression (11).

The majority of studies that investigated *TMPRSS2/ERG* rearrangement with FISH used dual-color *ERG* break-apart probes (12-16), which can identify the rearrangement or deletion of *ERG* gene but does not inform whether the rearranged *ERG* is fused with any 5'-partner. A few other studies utilized the tri-color fusion probes (6, 17-19), the application of which is usually challenged by possible overlap in excitation and/or emission wavelengths among different fluorochromes. The largest published study to date utilized a tri-color FISH assay by combining the red/green break-apart probe for *TMPRSS2* with an orange-labeled fusion probe for 3'*ERG* (18).

Here we report a novel 4-color FISH assay that overcomes common technical challenges and allows the detection of either *TMPRSS2* or *ERG* rearrangements regardless of the partner gene, a key advantage. The assay was successfully applied to frozen as well as FFPE prostate cancer samples, including primary cancer and castration-resistant (CRPC) metastatic tumors from patients and xenograft models with high sensitivity and specificity.

Materials and Methods

Sample source: cell lines, xenografts and patient tissues

The study was approved by the Institutional Review Boards at Fred Hutchinson Cancer Research Center (FHCRC) and the University of Washington (UW). LNCaP and VCaP were obtained from American Type Culture Collection (ATCC, VA). De-identified archived

primary prostate cancer samples were obtained from UW and Virginia Mason Hospital in Seattle. Prostate cancer xenografts were generated and maintained by the Vessella Lab at UW. Characteristic features of the xenografts have been described previously (20). Tissue microarrays (TMA) were generated from FFPE xenograft tissues as previously described (15). Metastatic CRPC tumor samples were collected from autopsies performed within 2 to 4 hours of death from 11 patients at UW under the rapid autopsy program (21). Tumors were obtained from various organ sites, frozen in OCT and stored at -80°C. All tissues were sectioned for H&E staining and verification of histology reviewed by a pathologist.

Metaphase harvest and karyotype analyses of prostate cancer cell lines and xenografts

LNCaP and VCaP cells were cultured in phenol-red free RPMI 1640 Medium and DMEM (Invitrogen, CA), respectively, supplemented with 10% fetal bovine serum (FBS, HyClone, Thermoscientific, MA) and 1% penicillin/streptomycin/L-glutamine at 37°C in a 5% CO_2 humidified incubator. Cells actively growing in logarithmic phase were incubated with colcemid at the final concentration of 0.04 μg/ml for 60 minutes at 37°C to arrest cells in meta phase. Cells were then treated with the pre-warmed hypotonic solution (0.075 M KCl) for 30 minutes before fixation in methanol and glacial acetic acid (2.5:1 ratio). Fixed cells were dropped on glass slides, treated with 0.025% trypsin in 0.9% NaCl, and stained with 1:4 diluted Wright's stain (pH 6.8) for GTW banding. Metaphases were analyzed under a microscope at a magnification of about 1250X for chromosome count and structural integrity. Karyotypes were written according to the ISCN2009 guideline. Metaphase nuclei were harvested from fresh prostate cancer xenografts in a similar way. Briefly, tumor tissues were thoroughly minced, treated with collagenase (2000 units/ml) to obtain single cell suspensions, which were then cultured in DMEM supplemented with 20% FBS and 1% penicillin/streptomycin/L-glutamine. Cells were allowed to grow for approximately 1 week before exposure to colcemid, followed by hypotonic treatment and fixation.

Fluorescent in Situ Hybridization (FISH)

Bacterial artificial chromosome (BAC) clones RP11-35C4, RP11-120C17, RP11-95I21, and RP11-476D17 received as gifts from Dr. Barbara Trask (FHCRC, WA) were used to generate probes targeting 5'-*TMPRSS2*, 3'-*TMPRSS2*, 5'-*ERG*, and 3'-*ERG*, respectively (Figure 1A). BAC DNA was extracted using procedures recommended by Children's Hospital Oakland Research Institute (CHORI, CA) and labeled with Nick Translation Kit (Abbott Molecular, IL, USA) using SpectrumRed-dUTP (5'-*TMPRSS2*), SpectrumGreen-dUTP (3'-*TMPRSS2*), SpectrumGold-dUTP (5'-*ERG*), and SpectrumAqua-dUTP (3'-*ERG*) (Abbott Molecular, IL). FISH analysis was performed according to standard procedures as published previously(22). Slides were examined for fusion/rearrangement and enumerated using AxioImager Z1/2 microscopes (Zeiss, Oberkochen, Germany) by two independent scientists. The proper localization of the probes on chromosome 21 was validated by metaphase FISH on normal human peripheral blood lymphocytes (Figure 1B). Sequence specificity of the BAC DNAs was also confirmed by PCR and Sanger sequencing (data not shown). Excluding tissues with unsatisfactory hybridization quality, a total of 59 primary cancer, 26 xenograft samples and 56 metastatic CRPC tumors were fully analyzed by FISH.

Reverse transcription (RT)-PCR and Gen-Probe analyses of *TMPRSS2:ERG* fusion

Total RNA was extracted from frozen tumor sections using RNeasy Mini Kit (Qiagen, MD). For each sample, 500 ng of RNA was converted to cDNA using SuperScript II Reverse Transcriptase (Life Technologies, CA) with an equal mixture of Random Primers (Life Technologies, CA) and Oligo dT (Integrated DNA Technologies, CA), and then amplified to detect the presence of *TMPRSS2:ERG* fusion transcript with the following primer set: Fwd 5'-AGC TAA GCA GGA GGC GGA-3' and Rev 5'-CGA CTG GTC CTC ACT CAC AA-3'.

Two or more 10-micron sections of frozen tissue were placed into an Aptima ® tube (Gen-Probe, CA) containing 3 mL of specimen transport medium. The tubes were heated for 30 minutes at 60C and stored at -80C. The samples were shipped to Gen-Probe. Target Capture RNA isolation, Transcription Mediated Amplification, and *TMPRSS2-ERG* fusion detection were performed by Gen-Probe as previously described (23). The primers span the junction between *TMPRSS2* exon 1 (NM_005656.3) and *ERG* exon 4 (NM_004449.4), producing an amplification product of 86 nucleotides.

Estimation of the performance characteristics of the 4-color FISH assay

Test sensitivity, specificity, positive/negative predictive value, and the estimated prevalence were calculated using the Clinical Calculator of VassarStats Website for Statistical Computation. Chi-square test was performed using GraphPad Prism.

Results

The novel 4-color FISH assay can detect multiple types of *TMPRSS2* and *ERG* rearrangements

The *TMPRSS2/ERG* rearrangement was examined by evaluating the number and the relative location of the 4 probes (Figure 1A) that target 5'-*TMPRSS2*, 3'-*TMPRSS2*, 5'-*ERG*, and 3'-*ERG* on chromosome 21 (Figure 1B) . The normal configuration was represented by the four probes adjacent to or overlapping with each other (Figure 1Ci), which are presented as two 4-color signal clusters in a diploid nucleus (Figure 1D) and three or more signal clusters in an aneuploid nucleus (Figure 1E). Pathologically benign prostate epithelia (n = 10) were used to establish false-positive cutoff values (mean ± 3SD) for various signal patterns on tissue. The typical *TMPRSS2:ERG* deletion fusion-positive tumors contain at least 50% scored nuclei demonstrating the juxtaposition of 5'-*TMPRSS2* (red) and 3'-*ERG* (aqua) with concurrent loss of the interstitial 3'-*TMPRSS2* (green) and 5'-*ERG* (gold) probes (Table 1 and Figure 1Cii, F, and G). Insertion or translocation, instead of deletion, of the interstitial region to a different genomic location results in an atypical fusion (Figure 1 Ciii and H). Importantly, our unique assay allowed for further categorization of *TMPRSS2* and *ERG* arrangement status beyond merely the presence or absence of gene fusion. When performed on tumor tissue specimens, the complex design of the 4-color FISH technique allowed for the revelation of various *TMPRSS2* and *ERG* signal configurations. In addition to the single deletion fusion and atypical fusion, the subclasses of fusion also include dual or multiple deletion fusion (Figure 1G and Table 1) and complex fusion with a mixture of different fusion and non-fusion alternative rearrangements. Among samples determined as fusion-negative, the assay detected the presence of normal alleles with two copies per nucleus (Figure 1D), copy number increase (CNI) of normal *TMPRSS2* and *ERG* (Figure 1E), and other alternative rearrangements, which include the 5'-*TMPRSS2* rearrangement showing individual red signal(s) dissociated from the adjacent green/gold/aqua probe signals (Figure 1Civ and I), and 3'-*ERG* rearrangement with individual aqua signal(s) separated from the adjacent red/green/gold probe signals (Figure 1Cv and J). In multiple tumors from one CRPC patient (#7), we also observed the separation of *TMPRSS2* (red/green) from *ERG* (gold/aqua) signals (Table 1 and Figure 1K).

Validation of the 4-color FISH assay on prostate cancer cell lines

We applied 4-color FISH on prostate cancer cell lines, LNCaP and VCaP, with known *TMPRSS2/ERG* rearrangement features (5). As expected, LNCaP cells were hypotetraploid without *TMPRSS2* or *ERG* rearrangements displaying 3 to 4 sets of normal *TMPRSS2* (red/green) and *ERG* (gold/ aqua) signals (Figure 2A). Metaphase-FISH further confirmed the presence of normal *TMPRSS2* and *ERG* signals on Chromosome 21 (Figure 2B). VCaP, a fusion-positive cell line, showed a clear *TMPRSS2:ERG* fusion signal pattern, as well as

additional *ERG* gene rearrangements (Figure 2C). VCaP contained three pairs of the normal *TMPRSS2* and *ERG*, shown as clusters of the four probes, and two fusion signals, demonstrated as juxtaposed 5'-*TMPRSS2* (red) and 3'-*ERG* (aqua) without the interstitial 3'-*TMPRSS2* (green) and 5'-*ERG* (gold) signals. In addition, alternative gene rearrangements were evident, including insertion/translocation of 3'-*TMPRSS2* (green) to chromosome 16 and insertion/translocation of 5'-*ERG* (gold) to chromosome 12 (Figure 2C and 2D).

Application of the 4-color FISH assay on primary and metastatic prostate cancer samples

Of 59 primary prostate cancer FFPE samples analyzed from 59 patients, 24 (41%) were positive for *TMPRSS2:ERG* fusion, including 3 (5.1%) with complex rearrangements and 1 (1.7%) with copy number increase (CNI) of the normal *TMPRSS2* and *ERG* loci in addition to fusion; 2 samples (3.3%) showed CNI of *TMPRSS2* and *ERG* without fusion; and 4 samples (7%) showed alternative rearrangements without *TMPRSS2:ERG* fusion. If we had used the common 2-color *ERG* break-apart probe, 2 of these 4 samples with 5'-*TMPRSS2* rearrangement would have been considered normal.

The 56 metastatic CRPC tumors and 26 xenograft samples (total n = 82) were derived from a total of 32 patients (Table 1 and 2). The 4-color FISH assay detected *TMPRSS2:ERG* fusion in 35 tumors (43%) from 10 patients (31%) with intra-patient heterogeneity. Among these, dual or multiple fusions (with or without additional normal copies) were present in 20 tumors (24%) from 5 patients (16%). The assay also detected alternative rearrangement without *TMPRSS2:ERG* fusion in 11 tumors (13%) from 5 patients (16%), which would have been called as normal by 2-color *ERG* break-apart FISH. Of CRPC samples, 20 tumors (24%) from 11 patients (34%) demonstrated CNI of both *TMPRSS2* and *ERG* without rearrangements. CRPC tissue types include frozen and FFPE sections. When both tissue types were available on the same sample, the results obtained from frozen tissues were consistent with those from FFPE tissues. In particular, the signal patterns observed from the tissue sections were consistent with those seen from intact cultured cells in the 4 xenograft lines described below.

Concordance between the 4- color FISH and RT-PCR/Gen-Probe Results

Concordant results were observed between the 4-color FISH findings and the *TMPRSS2:ERG* status defined by either Gen-Probe or RT-PCR analysis (Table 1), focusing on the fusion regardless of other types of rearrangements. The xenografts were generally evaluated using RT-PCR while the metastatic tumors were tested by Gen-Probe although some had both tests performed. Of 77 tumors with both FISH and Gen-Probe/RT-PCR data, 72 showed consistent data between FISH and the reference assay (93.5%), including 40 fusion-negative tumors and 32 tumors with *TMPRSS2:ERG* fusion. Two samples (2.6%), LuCaP23.12 and LuCaP23.1CR, which are derived from the same tumor, were presented as fusion positive by RT-PCR but not by FISH. Because *TMPRSS2:ERG* fusion was previously reported in LuCaP23.12 and LuCAP23.1(19, 24), this is considered false-negative result from the 4-color FISH assay. FISH, but not Gen-Probe assay, detected fusion in three tumors (4.0%), all of which were derived from patient #4, an individual with small cell carcinomas of the prostate. Previous studies have demonstrated in small cell carcinomas, even though *TMPRSS2:ERG* fusion is present at the genomic level, the *TMPRSS2:ERG* transcript is no longer expressed due to lack of AR or AR signaling that drives transcription expression (19, 25). Therefore, FISH results in patient #4 are considered true positives.

Therefore, using these modified RT-PCR/Gen-Probe results as a technical reference, the 4-color FISH assay has an analytical sensitivity of 94.5% (95% confidence interval [CI]

0.80-0.99) and a specificity of 100% (95% CI 0.89-1.00) for detecting *TMPRSS2:ERG* fusion. The positive predictive value is ~100% (95% CI 0.88-1.00), and the negative predictive value is 95.2% (95% CI 0.83-0.99). The predicted prevalence of the fusion detected by the 4-color FISH is 48.0% (95% CI 0.37-0.60).

Karyotype analysis of xenograft tissues

The complicated and potentially novel alternative gene rearrangements called for further characterization using karyotype analysis. Although the *TMPRSS2:ERG* fusion status has been reported previously for a few LuCaP xenografts(19), the extremely poor *in vitro* proliferative potential of the prostate cancer xenografts thwarted metaphase analysis for reliable karyotypes. We succeeded in karyotype analyses on four of the LuCaP xenograft tissues, including LuCaP 23.1, 35CR, 58, and 96 (Figure 3 and Table 2). Metaphase and interphase FISH analyses on short-term cultured xenograft cells confirmed alternative *TMPRSS2* rearrangement in LuCaP58 (Figure 3A) and LuCaP96 (Figure 3B), atypical fusion in LuCap35CR (Figure 3D), as well as the significant heterogeneity from cell to cell as observed during the FISH analysis on frozen and FFPE tissues (data not shown). Further characterization of the potential partner gene(s) of *TMPRSS2* in LuCaP58 and LuCaP96 ruled out two common ETS family members, *ETV1* and *ETV4*, as the rearrangement partner (data not shown).

Discussion

FISH detection of *TMPRSS2/ERG* rearrangements has the advantage of direct visualization of fusion or other rearrangement events within individual cells in the *in situ* tissue context. The novel 4-color FISH assay presents a robust tool for the detection of *TMPRSS2:ERG* fusion that was validated by alternative technologies. In order to identify rearrangements at both fusion gene partners, the 4-color FISH targets both the 5' and the 3' regions of *TMPRSS2* and *ERG*, respectively. The spectrally distinct fluorochromes used in our procedure showed little bleed-through across different wavelengths, allowing for a robust assay demonstrating a 94.5% analytical sensitivity and 100% specificity for detecting *TMPRSS2:ERG* fusion.

The 4-color FISH was successfully performed on frozen samples, FFPE samples, as well as tissue microarrays. The results are highly concordant with RT-PCR and karyotype analysis. In cases where data from frozen and FFPE-sections of the same samples were available, the 4-color FISH showed concordant results regardless of how the samples were preserved. A previous study has demonstrated the *TMPRSS2:ERG* fusion status in a subpopulation of the xenografts by RT-PCR(19). To demonstrate the technical reliability of the 4-color FISH, we compared its results with RT-PCR/Gen-Probe data obtained from corresponding samples and demonstrated a 93.5% concordant rate. Similar to previous findings, the 4-color FISH detected fusion in samples derived from small cell carcinoma, which was not consistently detectable by RT-PCR or Gen-Probe assay. Interestingly, all false negative samples, those fusion negative by FISH but positive by RT-PCR/Gen-Probe, were derived from the same original CRPC patient. To further understand the discrepancy, we carried out karyotype analysis on LuCaP23.1. Our karyotype analysis showed that LuCaP23.1 contains 4 copies of chromosome 21 per nucleus, each of which presents all four FISH signals. Therefore, although fusion transcript is detectable in the sample, genomic regions corresponding to 5'-*TMPRSS2*, 3'-*TMPRSS2*, 5'-*ERG*, and 3'-*ERG* all remain on chromosome 21. This is therefore a cryptic rearrangement.

The 4-color FISH assay not only identified *TMPRSS2:ERG* fusion at a rate similar to previous reports, but also provided researchers the opportunity to further classify fusions into multiple subtypes. Previous findings showed *ERG* rearrangements in 30-50% of

localized prostate cancer (5, 12, 15, 17, 18) and 40-50% among metastatic diseases (13, 18, 24, 26). In the majority of these studies, *TMPRSS2/ERG* rearrangements were identified via FISH that targeted either *ERG* only or both *TMPRSS2* and *ERG* but with independent hybridization on separate tissue sections. With this novel 4-color FISH assay reported here, which is capable of detecting rearrangements of *TMPRSS2* and *ERG* simultaneously in a single hybridization, we found rearrangements in 48% primary prostate cancer (including 41% demonstrating actual *TMPRSS2:ERG* fusion and 7% with alternative rearrangements) and in 57% CRPC metastatic tumors (including 43% *TMPRSS2:ERG* fusion and 13% alternative rearrangements), consistent with previous findings. Furthermore, the 4-color FISH also identified subtypes of fusion such as single or multiple deletion fusion and single or multiple insertion fusion. For example, the atypical fusion in LuCaP 35CR results from the insertion of the interstitial region between *TMPRSS2* and *ERG* to chromosome 3, which was validated in karyotype analysis. These characteristics enable researchers to compare disease outcomes among patients with different subtypes of fusions in future retrospective and prospective studies (12).

Besides the accurate detection of *TMPRSS2:ERG* fusion, the 4-color FISH demonstrated unique advantage in identifying multiple types of rearrangements other than *TMPRSS2:ERG* fusion, such as rearrangement of 5'-*TMPRSS2*, 3'-*TMPRSS3*, and 3'-*ERG*. Karyotype analysis further verified representative alternative rearrangements detected by 4-color FISH. In VCaP, aside from the fusion, the 3'-*TMPRSS2* is rearranged to chromosome 16, while the 5'-*ERG* is at chromosome 12. In LuCaP58 and LuCaP96, 5'-*TMPRSS2* is located at a chromosome separate from the 3'-*TMPRSS2* and the *ERG* locus. To the best of our knowledge, our study is the first to present karyotype results of multiple prostate xenografts, which contributes to further understanding of the complex genomic alternations in prostate tumors, especially in the context of whole genome and exome sequencing(3, 27). Additional alternative rearrangements of either *TMPRSS2* or *ERG* uniquely detected by this method may also suggest reflex testing for other less common *TMPRSS2* and *ERG* rearrangements, such as *TMPRSS2:ETV* fusions, and even allow for identification of potential novel partner genes of *TMPRSS2* or *ERG.* For instance, identification of potential partner gene of *TMPRSS2* on chromosome 16 and potential partner gene of *ERG* on chromosome 12 in the VCaP cell line will be a worthwhile future endeavor.

Variable degrees of difference in *TMPRSS2* and *ERG* rearrangements observed between primary prostate cancer and CRPC in our study is interesting. Even though the frequency of *TMPRSS2:ERG* fusion is similar in both the primary prostate cancer group and the CRPC group, complex or multiple *TMPRSS2:ERG* fusion, alternative rearrangement, as well as copy number increase (CNI) without rearrangement, all appeared to be more prevalent in CRPC than in the primary cancer cohort, suggesting a higher level of genomic complexity of CRPC clonal aberrations (Table 3). Multiple metastatic tumors from the same patient nevertheless showed similar *TMPRSS2* and *ERG* rearrangements for the most part. These results are consistent with the hypothesis that *TMPRESS:ERG* fusion is an early event during cancer development and likely facilitate prostate cancer progression (28). Further rearrangement or duplication of the *TMPRSS2:ERG* or individual genes, along with additional complex chromosomal translocations may take place as the disease progresses to the more advanced stage, particularly the castration resistant stage.

In conclusion, the current study demonstrated the development and validation of a novel 4-color FISH assay that can identify fusion as well as multiple types of *TMPRSS2* and *ERG* gene rearrangements with excellent sensitivity and specificity. It provides a powerful tool to study not merely *TMPRSS2:ERG* fusion, an important specific event in prostate cancer, but

also its subtypes and related rearrangements, in the context of prostate cancer pathogenesis and prognosis.

Acknowledgments

We thank Holly Nguyen for maintenance of the xenograft lines and providing specimens, Dr. Colm Morrisey for sectioning the tissue microarray blocks, and Melissa Chiu for PCR and sequencing verification of BAC clones. We also thank Meg Bender and Stacie Thomas for clerical assistance.

This study is supported by PNW SPORE P50 CA097186 and P01 CA 085859 from the National Cancer Institute, and by Richard M Lucas Foundation (for the xenograft generation and clinical specimens).

REFERENCES

1. Shah RB, Chinnaiyan AM. The discovery of common recurrent transmembrane protease serine 2 (TMPRSS2)-erythroblastosis virus E26 transforming sequence (ETS) gene fusions in prostate cancer: significance and clinical implications. Adv Anat Pathol. 2009; 16:145–153. [PubMed: 19395877]
2. Brenner JC, Feng FY, Han S, Patel S, Goyal SV, Bou-Maroun LM, Liu M, Lonigro R, Prensner JR, Tomlins SA, Chinnaiyan AM. PARP-1 inhibition as a targeted strategy to treat Ewing's sarcoma. Cancer Res. 2012; 72:1608–1613. [PubMed: 22287547]
3. Berger MF, Lawrence MS, Demichelis F, Drier Y, Cibulskis K, Sivachenko AY, Sboner A, Esgueva R, Pflueger D, Sougnez C, Onofrio R, Carter SL, Park K, Habegger L, Ambrogio L, Fennell T, Parkin M, Saksena G, Voet D, Ramos AH, Pugh TJ, Wilkinson J, Fisher S, Winckler W, Mahan S, Ardlie K, Baldwin J, Simons JW, Kitabayashi N, MacDonald TY, Kantoff PW, Chin L, Gabriel SB, Gerstein MB, Golub TR, Meyerson M, Tewari A, Lander ES, Getz G, Rubin MA, Garraway LA. The genomic complexity of primary human prostate cancer. Nature. 2011; 470:214–220. [PubMed: 21307934]
4. Teixeira MR. Chromosome mechanisms giving rise to the TMPRSS2-ERG fusion oncogene in prostate cancer and HGPIN lesions. Am J Surg Pathol. 2008; 32:642–644. author reply 644. [PubMed: 18317354]
5. Tomlins SA, Rhodes DR, Perner S, Dhanasekaran SM, Mehra R, Sun XW, Varambally S, Cao X, Tchinda J, Kuefer R, Lee C, Montie JE, Shah RB, Pienta KJ, Rubin MA, Chinnaiyan AM. Recurrent fusion of TMPRSS2 and ETS transcription factor genes in prostate cancer. Science. 2005; 310:644–648. [PubMed: 16254181]
6. Rajput AB, Miller MA, De Luca A, Boyd N, Leung S, Hurtado-Coll A, Fazli L, Jones EC, Palmer JB, Gleave ME, Cox ME, Huntsman DG. Frequency of the TMPRSS2:ERG gene fusion is increased in moderate to poorly differentiated prostate cancers. J Clin Pathol. 2007; 60:1238–1243. [PubMed: 17259299]
7. Clark JP, Cooper CS. ETS gene fusions in prostate cancer. Nat Rev Urol. 2009; 6:429–439. [PubMed: 19657377]
8. Zhang S, Pavlovitz B, Tull J, Wang Y, Deng FM, Fuller C. Detection of TMPRSS2 gene deletions and translocations in carcinoma, intraepithelial neoplasia, and normal epithelium of the prostate by direct fluorescence in situ hybridization. Diagn Mol Pathol. 2010; 19:151–156. [PubMed: 20736744]
9. Tomlins SA, Bjartell A, Chinnaiyan AM, Jenster G, Nam RK, Rubin MA, Schalken JA. ETS gene fusions in prostate cancer: from discovery to daily clinical practice. Eur Urol. 2009; 56:275–286. [PubMed: 19409690]
10. Furusato B, Tan SH, Young D, Dobi A, Sun C, Mohamed AA, Thangapazham R, Chen Y, McMaster G, Sreenath T, Petrovics G, McLeod DG, Srivastava S, Sesterhenn IA. ERG oncoprotein expression in prostate cancer: clonal progression of ERG-positive tumor cells and potential for ERG-based stratification. Prostate cancer and prostatic diseases. 2010; 13:228–237. [PubMed: 20585344]
11. Park K, Tomlins SA, Mudaliar KM, Chiu YL, Esgueva R, Mehra R, Suleman K, Varambally S, Brenner JC, MacDonald T, Srivastava A, Tewari AK, Sathyanarayana U, Nagy D, Pestano G,

Kunju LP, Demichelis F, Chinnaiyan AM, Rubin MA. Antibody-based detection of ERG rearrangement-positive prostate cancer. Neoplasia. 2010; 12:590–598. [PubMed: 20651988]

12. Attard G, Clark J, Ambroisine L, Fisher G, Kovacs G, Flohr P, Berney D, Foster CS, Fletcher A, Gerald WL, Moller H, Reuter V, De Bono JS, Scardino P, Cuzick J, Cooper CS. Duplication of the fusion of TMPRSS2 to ERG sequences identifies fatal human prostate cancer. Oncogene. 2008; 27:253–263. [PubMed: 17637754]
13. Mehra R, Tomlins SA, Shen R, Nadeem O, Wang L, Wei JT, Pienta KJ, Ghosh D, Rubin MA, Chinnaiyan AM, Shah RB. Comprehensive assessment of TMPRSS2 and ETS family gene aberrations in clinically localized prostate cancer. Mod Pathol. 2007; 20:538–544. [PubMed: 17334343]
14. Demichelis F, Fall K, Perner S, Andren O, Schmidt F, Setlur SR, Hoshida Y, Mosquera JM, Pawitan Y, Lee C, Adami HO, Mucci LA, Kantoff PW, Andersson SO, Chinnaiyan AM, Johansson JE, Rubin MA. TMPRSS2:ERG gene fusion associated with lethal prostate cancer in a watchful waiting cohort. Oncogene. 2007; 26:4596–4599. [PubMed: 17237811]
15. Esgueva R, Perner S, C JL, Scheble V, Stephan C, Lein M, Fritzsche FR, Dietel M, Kristiansen G, Rubin MA. Prevalence of TMPRSS2-ERG and SLC45A3-ERG gene fusions in a large prostatectomy cohort. Mod Pathol. 2010; 23:539–546. [PubMed: 20118910]
16. Lee K, Chae JY, Kwak C, Ku JH, Moon KC. TMPRSS2-ERG gene fusion and clinicopathologic characteristics of Korean prostate cancer patients. Urology. 2010; 76:1268, e1267–1213. [PubMed: 20800881]
17. FitzGerald LM, Agalliu I, Johnson K, Miller MA, Kwon EM, Hurtado-Coll A, Fazli L, Rajput AB, Gleave ME, Cox ME, Ostrander EA, Stanford JL, Huntsman DG. Association of TMPRSS2-ERG gene fusion with clinical characteristics and outcomes: results from a population-based study of prostate cancer. BMC Cancer. 2008; 8:230. [PubMed: 18694509]
18. Gopalan A, Leversha MA, Satagopan JM, Zhou Q, Al-Ahmadie HA, Fine SW, Eastham JA, Scardino PT, Scher HI, Tickoo SK, Reuter VE, Gerald WL. TMPRSS2-ERG gene fusion is not associated with outcome in patients treated by prostatectomy. Cancer Res. 2009; 69:1400–1406. [PubMed: 19190343]
19. Saramaki OR, Harjula AE, Martikainen PM, Vessella RL, Tammela TL, Visakorpi T. TMPRSS2:ERG fusion identifies a subgroup of prostate cancers with a favorable prognosis. Clin Cancer Res. 2008; 14:3395–3400. [PubMed: 18519769]
20. Corey, EV,R. Xenograft Models of Human Prostate Cancer.. In: Chung LWK, IW.; Simons, JW., editors. Contemporary Cancer Research: Prostate Cancer: Biology, Genetics, and the New Therapeutics. Vol. I. Humana Press; Totowa: 2007. p. 3-31.
21. Morrissey C, True LD, Roudier MP, Coleman IM, Hawley S, Nelson PS, Coleman R, Wang YC, Corey E, Lange PH, Higano CS, Vessella RL. Differential expression of angiogenesis associated genes in prostate cancer bone, liver and lymph node metastases. Clin Exp Metastasis. 2008; 25:377–388. [PubMed: 17972146]
22. Ronski K, Sanders M, Burleson JA, Moyo V, Benn P, Fang M. Early growth response gene 1 (EGR1) is deleted in estrogen receptor-negative human breast carcinoma. Cancer. 2005; 104:925–930. [PubMed: 15999367]
23. Groskopf J, Aubin SM, Deras IL, Blase A, Bodrug S, Clark C, Brentano S, Mathis J, Pham J, Meyer T, Cass M, Hodge P, Macairan ML, Marks LS, Rittenhouse H. APTIMA PCA3 molecular urine test: development of a method to aid in the diagnosis of prostate cancer. Clin Chem. 2006; 52:1089–1095. [PubMed: 16627561]
24. Perner S, Demichelis F, Beroukhim R, Schmidt FH, Mosquera JM, Setlur S, Tchinda J, Tomlins SA, Hofer MD, Pienta KG, Kuefer R, Vessella R, Sun XW, Meyerson M, Lee C, Sellers WR, Chinnaiyan AM, Rubin MA. TMPRSS2:ERG fusion-associated deletions provide insight into the heterogeneity of prostate cancer. Cancer Res. 2006; 66:8337–8341. [PubMed: 16951139]
25. Hermans KG, van Marion R, van Dekken H, Jenster G, van Weerden WM, Trapman J. TMPRSS2:ERG fusion by translocation or interstitial deletion is highly relevant in androgen-dependent prostate cancer, but is bypassed in late-stage androgen receptor-negative prostate cancer. Cancer Res. 2006; 66:10658–10663. [PubMed: 17108102]
26. Holcomb IN, Young JM, Coleman IM, Salari K, Grove DI, Hsu L, True LD, Roudier MP, Morrissey CM, Higano CS, Nelson PS, Vessella RL, Trask BJ. Comparative analyses of

chromosome alterations in soft-tissue metastases within and across patients with castration-resistant prostate cancer. Cancer Res. 2009; 69:7793–7802. [PubMed: 19773449]

27. Kumar A, White TA, MacKenzie AP, Clegg N, Lee C, Dumpit RF, Coleman I, Ng SB, Salipante SJ, Rieder MJ, Nickerson DA, Corey E, Lange PH, Morrissey C, Vessella RL, Nelson PS, Shendure J. Exome sequencing identifies a spectrum of mutation frequencies in advanced and lethal prostate cancers. Proc Natl Acad Sci U S A. 2011; 108:17087–17092. [PubMed: 21949389]
28. Perner S, Mosquera JM, Demichelis F, Hofer MD, Paris PL, Simko J, Collins C, Bismar TA, Chinnaiyan AM, De Marzo AM, Rubin MA. TMPRSS2-ERG fusion prostate cancer: an early molecular event associated with invasion. Am J Surg Pathol. 2007; 31:882–888. [PubMed: 17527075]

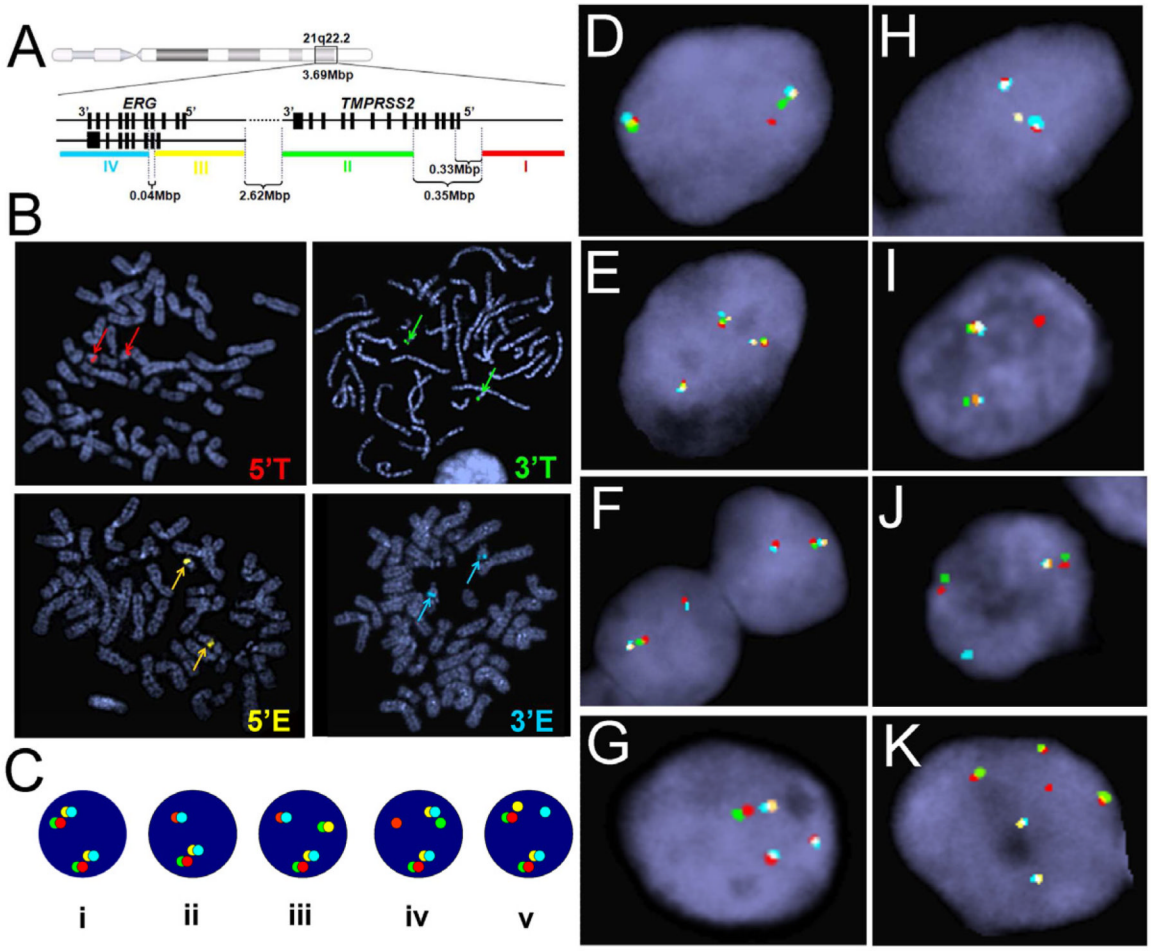

Figure 1.

The novel 4-color FISH technique for the detection of rearrangements of *TMPRSS2* and/or *ERG*. (A) The FISH technique involved hybridization of samples with four probes, 5'-*TMPRSS2* (red, probe I), 3'-*TMPRSS2* (green, probe II), 5'-*ERG* (gold, probe III), and 3'-*ERG* (aqua, probe IV) simultaneously. (B) Metaphases prepared from normal human peripheral blood lymphocytes were used to validate proper localization of FISH probes. Red, green, gold, and aqua probes, targeting 5'- *TMPRSS2*, 3'-*TMPRSS2*, 5'-*ERG*, and 3'-*ERG*, respectively, all located to chromosome 21. Color arrows point to the location of the corresponding FISH signals. (C) Illustration of multiple types of signal patterns detected by 4-color FISH. (D-K) Representative FISH images of tumor cells: (Ci and D) normal; (E) copy number increase (CNI) of normal *TMPRSS2* and *ERG*; (Cii and F) single deletion fusion; (G) dual deletion fusion; (Ciii and H) atypical fusion; (Civ and I) rearrangement of 5'-*TMPRSS2*; (Cv and J) rearrangement of 3'-*ERG*; and (K) separation of *TMPRSS2* from *ERG* signals.

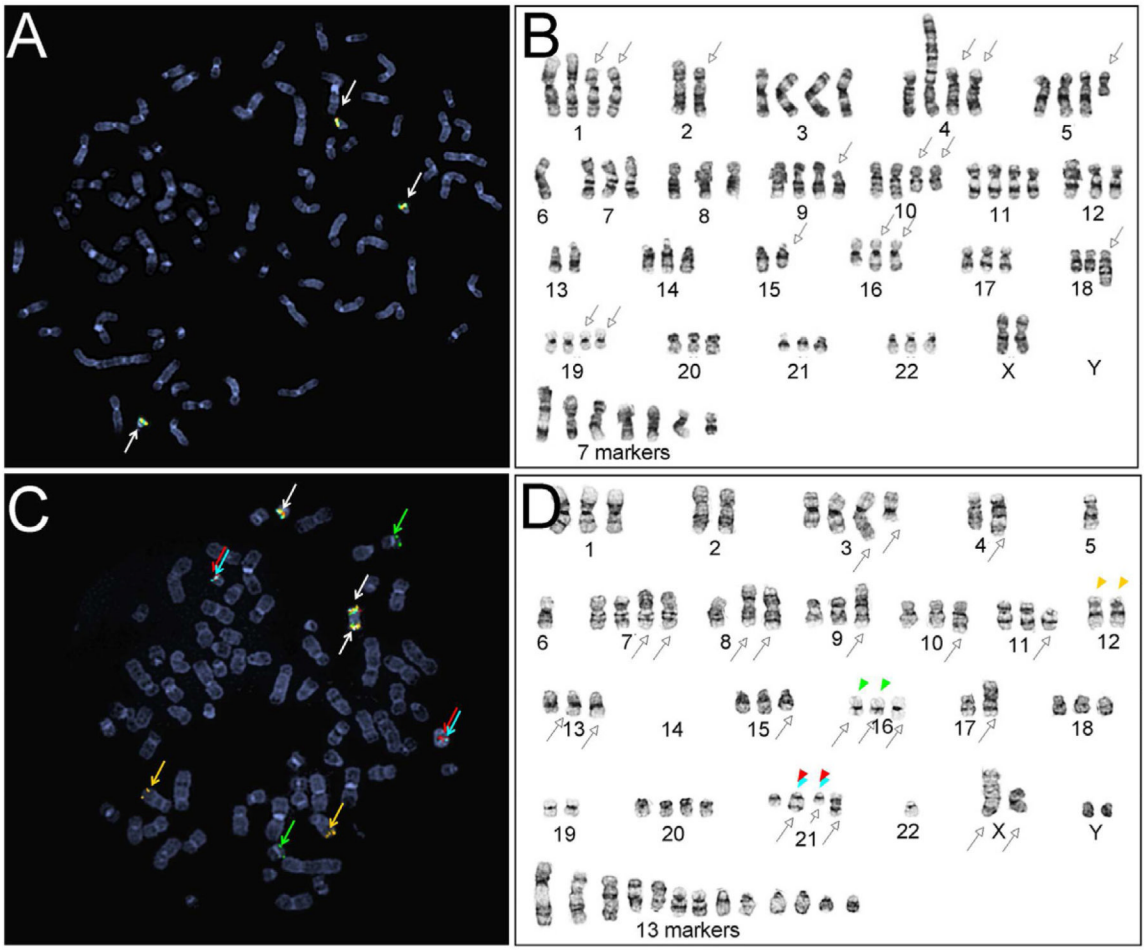

Figure 2.

Characterization of *TMPRSS2* and *ERG* rearrangement patterns in prostate cancer cell lines determined by the 4-color FISH assay. (A and B) Metaphase FISH and karyogram images from fusion-negative LNCaP; (C and D) Metaphase FISH and karyogram images of fusion-positive VCap. White arrows indicate normal FISH signals, represented as clusters of the 4 probes. Empty arrows with black outline indicate abnormal chromosomes identified during karyotype analysis. Red, green, gold, and aqua arrow or arrow heads highlight positions of FISH signals corresponding to 5'-*TMPRSS2*, 3'-*TMPRSS2*, 5'-*ERG* and 3'-*ERG*.

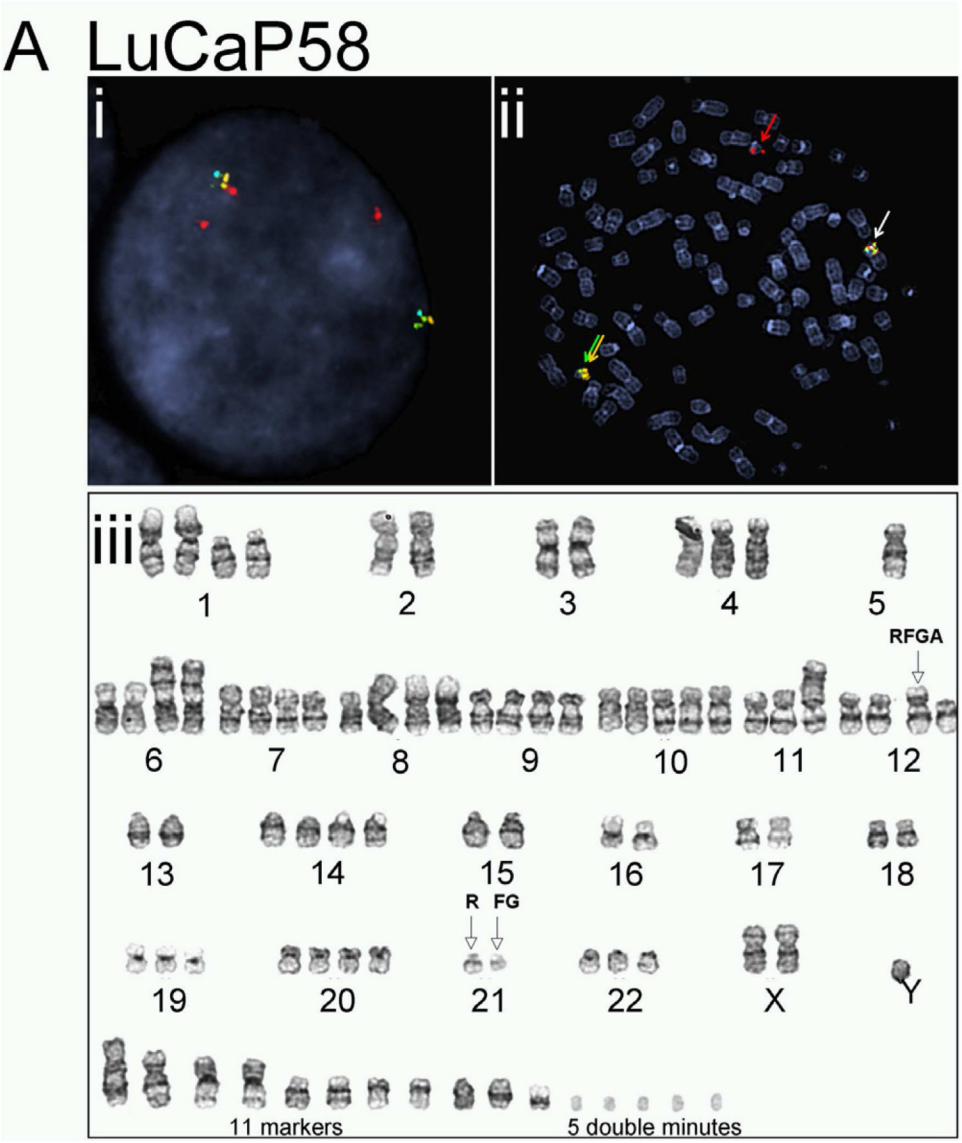

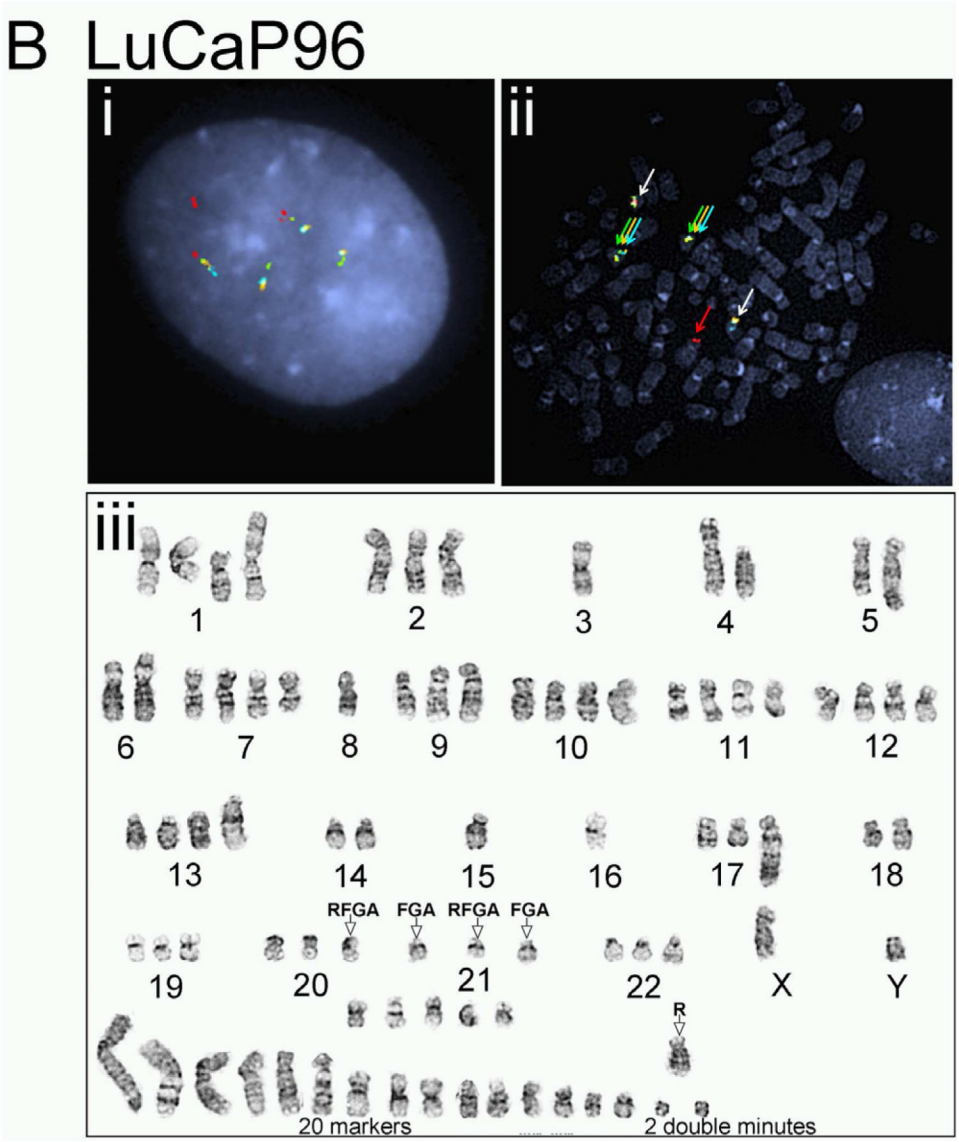

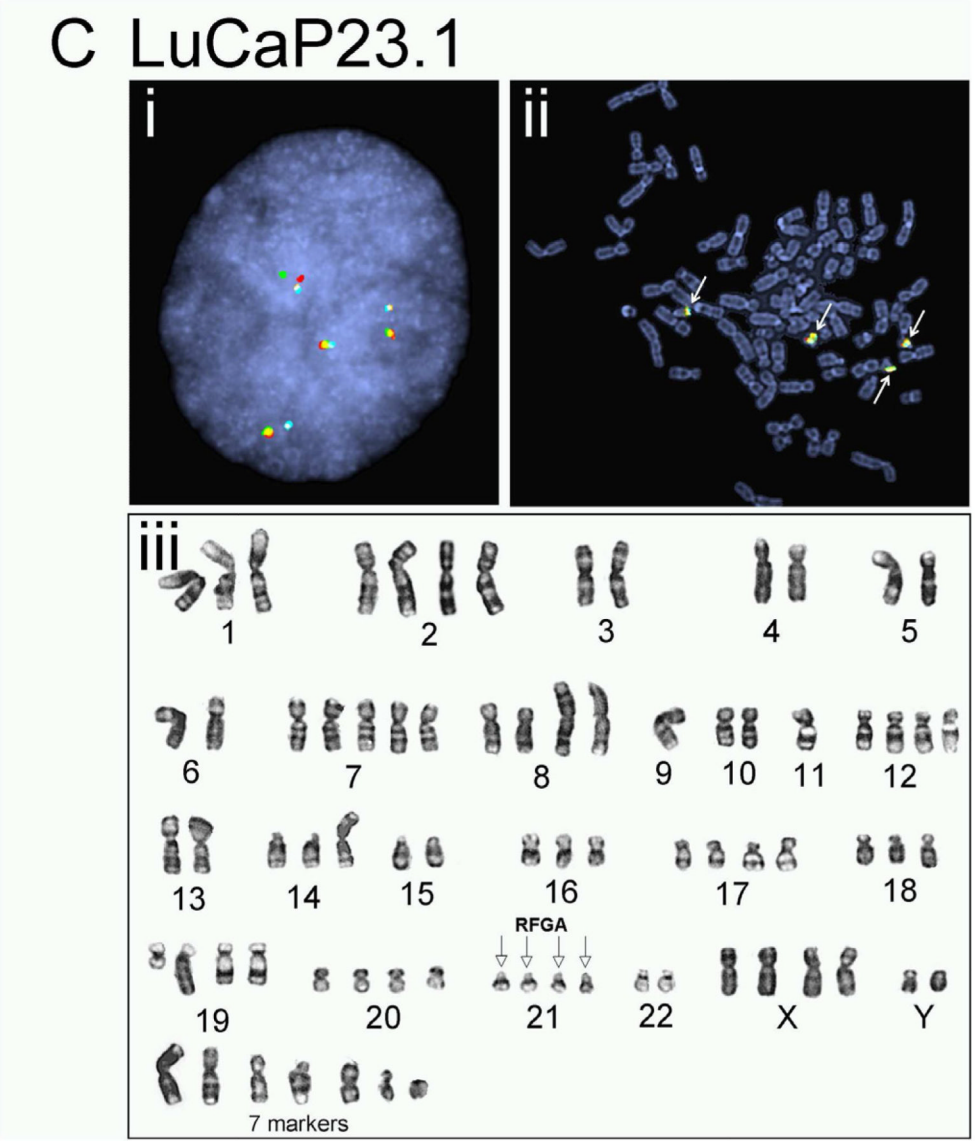

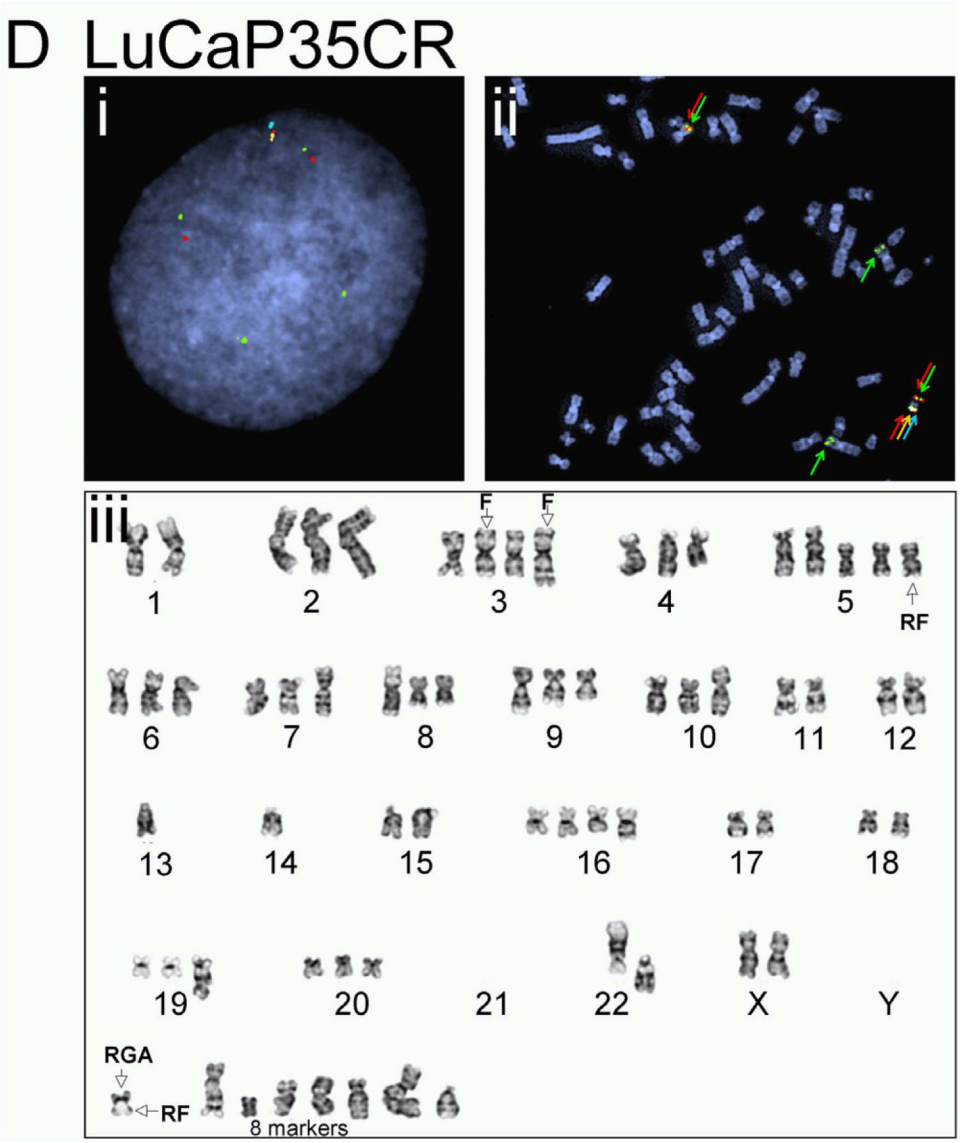

Figure 3.

Karyotype analysis and corresponding FISH results on prostate cancer xenografts. LuCaP 58 (A), 96 (B), 23.1 (C), and 35CR (D). Representative interphase FISH images obtained from intact nuclei are shown in (i) of each panel; metaphase FISH images are presented in (ii). Karyogram images are in (iii). Red (R), green (F), gold (G), and aqua (A) arrows in FISH images highlight positions of FISH signals corresponding to 5'-*TMPRSS2*, 3'-*TMPRSS2*, 5'-*ERG* and 3'-*ERG*. Empty arrows with black outline in karyograms highlight the position of indicated signal(s) on a given chromosome.

Table 1

Results of *TMPRSS2* and *ERG* rearrangement with the novel 4-color FISH assay on castration resistant prostate cancer samples, including metastasis

Patient	Tissue	*TMPRSS2:ERG* fusion			Alternative rearrangement	CNI	Normal result	Concordance with RT-PCR/Gen-Probe
		Single (del)	Multiple (del)	Atypical				
9	Adrenal1	38%	56%					Y
9	Adrenal2	38%	52%					Y
9	Liver	64%	10%					Y
9	LN1	22%	44%					Y
9	LN2	30%	54%					Y
9	LN3	34%	24%					Y
9	LN4	32%	14%					Y
9	Lung1	32%	54%					Y
9	Lung2	22%	66%					Y
9	Spleen	40%	14%					Y
9	Prostate	32%	20%					Y
5	LN1	12%	80%					Y
5	LN2		100%					Y
5	LN3	20%	78%					Y
5	LN4	24%	72%					Y
5	LN5	12%	88%					Y
5	Prostate	84%	12%					Y
4	Liver	92%						Y
4	LN1	96%						N**
4	Lung1	96%						N**
4	Spleen	92%	8%					N**
2	LN1			88%				Y
2	LN2			97%				Y
2	LN3			100%				Y
2	Lung1			79%				Y
2	Lung2			88%				Y
2	Prostate			74%				Y
7	LN1				67%	20%		NA
7	LN2				89%			NA
7	LN3				84%			Y
7	LN4				97%			Y

Patient	Tissue	*TMPRSS2:ERG* fusion			Alternative rearrangement	CNI	Normal result	Concordance with RT-PCR/Gen-Probe
		Single (del)	Multiple (del)	Atypical				
7	Prostate				92%			Y
11	LN1					72%		Y
11	LN3					48%		Y
11	Prostate 1				78%			Y
11	Prostate 2				74%			Y
6	LN1					100%		Y
6	LN2					82%		Y
6	LN3					78%		Y
6	Peritoneal					92%		Y
1	Liver					12%		Y
1	LN1						Normal	Y
1	LN2						Normal	Y
1	Prostate					24%		Y
3	Liver					34%		Y
3	LN1					74%		Y
3	LN2					80%		Y
3	Lung					59%		Y
3	Prostate 1						Normal	Y
3	Prostate 2						Normal	Y
8	Liver						Normal	Y
8	LN1						Normal	Y
8	LN2						Normal	Y
8	LN3						Normal	Y
8	Lung						Normal	Y
8	Prostate						Normal	Y
LuCaP49[a]	Omental fat	86%						N/Y
LuCaP86.2	Bladder	62%				16%		Y
LuCaP93[a]	Prostate	60%	36%					Y
LuCaP145.1[a]	Liver	94%						Y
LuCaP145.2[a]	LN	14%	86%					Y
LuCaP35	LN			100%				Y
LuCaP35CR	LN			100%				Y
LuCaP92.1	Peritoneum			100%				Y

Cancer Genet. Author manuscript; available in PMC 2014 January 24.

Patient	Tissue	*TMPRSS2:ERG* fusion			Alternative rearrangement	CNI	Normal result	Concordance with RT-PCR/Gen-Probe
		Single (del)	Multiple (del)	Atypical				
LuCaP58	LN				86%			Y
LuCaP96	Prostate				80%	26%		Y
LuCaP96CR	Prostate				98%	38%		Y
LuCaP146[b]	NA				92%	28%		NA
LuCaP23.12	Liver					50%		N
LuCaP23.1CR	LN					60%		N
LuCaP69[b]	NA					62%		NA
LuCaP70	Liver					64%		Y
LuCaP73	Prostate					60%		Y
LuCaP105	Rib					16%		Y
LuCaP115	LN					24%		Y
LuCaP141	Prostate					34%		Y
LuCaP77	Femur						Normal	Y
LuCaP78	Peritoneum						Normal	Y
LuCaP81	LN						Normal	Y
LuCaP136	Acites fluid (cells)						Normal	Y
LuCaP147	Liver						Normal	Y
LuCaP153[b]	NA						Normal	NA

CR Castration resistant; these xenograft lines used to have the name suffix as “v” or “ai”

LN Lymph node

NA Data not available

[a]Small cell carcinoma samples; discrepancy between FISH and RT-PCR in some (**) was documented previously (Saramäki et al., 2008). Therefore, fusion detected by FISH is considered as true positive.

[b]Xenograft discontinued Blank indicates the corresponding FISH pattern was absent from the sample or below threshold

Table 2

Karyotype results of prostate cancer cell lines and xenografts

Cell line/xenograft	Karyotype
LNCaP	78~79,XX,-Y,-Y,add(1)(p22)x2,-2,add(2)(p11.2)x2,add(4)(p14),add(4)(q31)x2,del(5)(q14),-6,-6,-6,-7,-8, add(8)(p11.2),add(9)(p13),add(10)(q22)x2,-12,-13,-13,-14,-15,-15, del(15)(q22q24),-16,add(16)(q12)x2,-17,-17,-18,add(18)(q23),del(19)(q13.1q13.1)x2,-21,-22,+6~7mar
VCaP	73,YY,add(X)(q22),del(X)(q22),-1,-2,-2,add(3)(q21),del(3)(q12),-4,-4,add(4)(q21),-5,-5,-5,-6,-6,-6,add(7)(p13),add(7)(p15), -8,add(8)(p11.2),add(8)(p21),-9,add(9)(p24),-10,add(10)(q24),del(11)(p11.2),-12,-12,add(12)(q24.1)x2,-13,add(13)(q32)x2,-14,-14,-14,-14, -15,del(15)(q22),-16,del(16)(q13)x2,i(16)(p10),-17,-17,add(17)(p11.2),-18,-19,-19,add(21)(q22),del(21)(q22),i(21)q10),-22,-22,-22,+13mar
LuCaP 23.1	76<4n>,XXYY,+X,+X,-1,inv(2)(q13q31)x2,-3,-3,-4,-4,-5,-5,add(5)(p15),add(5)(q11.2),-6,-6,+7,i(8)(q10)x2, -9,-9,-9,-10,-10,-11,-11,-11,-13,-13,add(13)(p11.2)x2,-14,i(14)(q10), -15,-15,-16,-18,add(19)(q13.1),der(19)t(11;19)(q13;q13.3)x2,-22,-22,+7mar
LuCaP 35CR	66<3N>,XX,-Y,-1,add(1)(q32),del(1)(q32),?2,der(2)add(2)(p13)add(2)(q21),+add(3)(q21),add(3)(q21),del(3)(q21q23)x2,add(4)(p14),add(4)(q12), +5x2,add(5)(q13),del(5)(q13q31)x2,add(7)(p13),add(8)(p11.2),del(8)(q13q22)x2,add(9)(q13),add(10)(p11.2),der(10)add(10)(p13)add(10)(q22),-11, -12,add(12)(p11.2),-13x2,14x2,-15,add(15)(p11.2),+16,add(16)(q24),del(16)(q24),-17,-18,add(19)(q13.1),-21x3,-22,add(22)(p11.2),add(22)(q13),+8mar
LuCaP 58	76~80<4n>,XXY,-Y,add(1)(p13)x2,-2,-2,-2,-3,-3,-4,-5,-5,-5,add(6)(p23)x2,der(7)add(7)(p11.2)del(7)(q11.2q22)x2, add(8)(p11.2), der(8)t(1 ;8)(p22;p11.2)x2,+10,add(10)(q11.2)x2,-11,add(11)(p11.2),del(12)(p11.2),der(12)t(12;21)(p11.2;q11.2),-13,-13,-15, -15,-16,-16,-17,-17,-18,-18,-19,-21,-21,del(21)(q11.2q22),-22,+9~11mar,3~5dmin
LuCaP 96	82,XY,-X,-Y,add(1)(p13),der(1)add(1)(p13)add(1)q21),-2,-3,-3,-3,-4,-4,add(4)(p14),del(4)(p14p16),-5,-5,add(5)(q31),-6,-6,add(6)(p25), add(7)(p15),del(7)(q22q32),-8,-8,-8,-9,add(9)(q22),add(9)(q13),add(10)(q22), add(10)(q26),del(11)(q21q23)x3,add(12)(q13),add(13)(q32),-14,-14,-15,-15,-15,-16,-16,-16,-17,add(17)(q21),-18,-18,add(18)(q21),-19, -20,der(20)t(20;21)(p11.2;q22),-21,add(21)(q22),-22,add(22)(q13),+21mar,2dmin

Table 3

Differences in the abnormalities detected by the 4-color *TMPRSS2/ERG* FISH between primary prostate cancer and castration resistant cancer

	Primary tumors		CRPC tumors	
	N	**%**	**N**	**%**
Total	59		82	
TMPRSS2:ERG fusion	24	41%	35	43%
Single (del)	*13*	*22%*	*6*	*7%*
Multiple (del)	*0*	*0%*	*20*	*24%*
Atypical	*11*	*19%*	*9*	*11%*
Alternative rearrangement	4	7%	11	13%
CNI	2	3%	20	24%
Normal	29	49%	16	20%

Only samples successfully hybridized were presented.

Chi-square test results: Chi squared = 115.8, $P < 0.0001$